

Poly(bisthiophene-carbazole-fullerene) Double-Cable Polymer As New Donor–acceptor Material: Preparation and Electrochemical and Spectroscopic Characterization

Nicolas Berton, Isabelle Fabre-Francke, David Bourrat, Frédéric Chandezon,* and Saïd Sadki*

INAC, UMR 5819-SPRAM (CEA-CNRS-Univ. J. Fourier-Grenoble I), Laboratoire d'Electronique Moléculaire Organique et Hybride, CEA Grenoble, 17 Rue des Martyrs 38054 Grenoble Cedex 9, France

Received: June 23, 2009; Revised Manuscript Received: September 14, 2009

A new donor–acceptor dyad, namely, a 3,6-bis(thiophen-2-yl)carbazole derivative bearing a C₆₀ fullerene as a side group (BTC-F), was prepared and characterized. Electropolymerization of BTC-F leads to the formation of a donor–acceptor double-cable polymer (PBTC-F) with high fullerene content (63 wt %) corresponding to one C₆₀ per polymer repeat unit. The electronic properties of BTC-F and PBTC-F were studied by electrochemical and spectroscopic techniques. Photoluminescence quenching is observed in diluted solutions of BTC-F compared to the nongrafted monomer BTC indicating that an intramolecular charge transfer takes place between the two components of the dyad. The positions of the HOMO and LUMO levels of the monomer and the polymer were accurately determined by differential pulse voltammetry (DPV). The LUMO energy level of the fullerene moiety in BTC-F lies at 3.7 eV below the vacuum level, i.e., slightly higher than corresponding levels of C₆₀ and PCBM. DPV characterization of PBTC-F indicates little ground state interaction between the π -conjugated main chain and the C₆₀ side groups and a high donor HOMO–acceptor LUMO gap of 1.47 eV.

Introduction

Conjugated polymers based on carbazole derivatives are materials which have generated increasing interest in the past years for organic electronics applications due to their electroluminescence,¹ thermoelectrical,² and hole-transport properties.³ Polycarbazole derivatives were therefore used as hole-transporting materials in organic light-emitting diodes⁴ and active layers in p-channel organic field-effect transistors.⁵ They are also attractive for polymer-based photovoltaic applications because of their good photoconductive properties when blended with fullerenes.⁶ Due to a relatively low position of their highest occupied molecular orbital level (HOMO), polycarbazoles are air-stable materials. This proves to be a significant advantage compared to the presently most popular material in the field, i.e., poly(3-hexylthiophene) (P3HT). Polycarbazole-based solar cells show higher open-circuit voltage (V_{oc}) compared to P3HT,⁷ in accordance with the fact that the V_{oc} of operating photovoltaic devices is determined by the difference between the HOMO of the donor and the lowest unoccupied molecular orbital (LUMO) of the acceptor.⁸ Recently, poly(thiophene-carbazole) derivatives have proven to be good candidates for the design of highly efficient polymers with high hole mobility and optimized HOMO and LUMO (lowest unoccupied molecular orbital) energy levels for photovoltaic applications. Power conversion efficiencies (PCE) up to 6% were obtained using such systems with 1-(3-methoxycarbonyl)propyl-1-phenyl [6,6]C₆₁ (PCBM) or the C₇₀ equivalent, namely, PC₇₀BM, as the electron acceptor.⁹

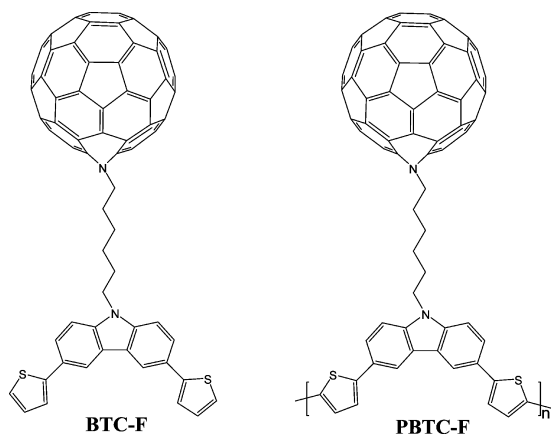
For such applications, an efficient design is the bulk heterojunction scheme where the two partners, the polymer (electron donor) and the electron acceptor (PCBM or PC₇₀BM), form percolating networks interpenetrated at the nanoscale. One major issue usually associated with the bulk heterojunction structure remains the control of the phase separation between the polymer

donor and the fullerene-based acceptor: for an efficient photo-induced charge separation and the subsequent transport of the free hole and electron, respectively, to the cathode and the anode, the optimal length scale of the phase separation between the two components of the blend should be close to the diffusion length of the excitons in the absorbing π -conjugated polymer phase, i.e., around 10 nm.¹⁰ To address this problem, the grafting of fullerenes as side groups on the polymer backbone was proposed.^{11–13} Such so-called “double-cable” polymers can be obtained by chemical polymerization or by electropolymerization of monomer–fullerene dyads.^{14–18} The double-cable structure guarantees the proximity of the donor and of the acceptor units, and it has indeed shown a capacity to limit phase separation compared with a simple blend.¹⁴ However, to date, double-cable polymers have given poor to moderate power conversion efficiencies (PCE). This was attributed to an insufficient fullerene loading in the material.^{18–20}

The electropolymerization of fullerene-containing monomers should enable the formation of films of double-cable polymers with a sufficiently high fullerene ratio despite the low solubility or even insolubility of such polymers. In particular, films of polycarbazole-based double-cable polymers, electrodeposited on a suitable transparent electrode, should in principle lead to solar cells with high V_{oc} and PCE provided that the specific electronic properties of the polymer and the acceptor parts are preserved within the double-cable structure.

In this work, we report the synthesis of a new donor–acceptor dyad, namely, *N*-(6-azafullerohexane)-3,6-bis(thiophen-2-yl)-carbazole (BTC-F). The electropolymerization of the BTC-F monomer unit leads to the formation of thin films of the double-cable polymer PBTC-F bearing one C₆₀ per polymer repeat unit corresponding to a fullerene content of 63 wt % (Scheme 1). Any organic electronics application of new materials requires the detailed determination of their optical, electronic, and redox properties. For these reasons, detailed investigations of BTC-F and PBTC-F were undertaken by means of UV–vis absorption

* Corresponding authors. E-mail: frederic.chandezon@cea.fr; said.sadki@cea.fr.

SCHEME 1: Chemical Structures of BTC-F and PBTC-F


and photoluminescence spectroscopies, cyclic voltammetry (CV), and differential pulse voltammetry (DPV). This gave us access to the HOMO and LUMO levels of the compounds. Moreover, it provided information concerning the intramolecular interactions between the electron-donor BTC conjugated unit and the electron-acceptor fullerene. The results show a favorable stacking of the HOMO–LUMO energy levels between the fullerene moieties and the π -conjugated chain for intramolecular charge transfer.

Experimental Section

General. Tetrabutylammonium perchlorate (Fluka), synthesis grade dichloromethane (CH_2Cl_2) (SDS, purex), *N,N*-dimethylformamide (DMF) (Carlo Erba, RPE), ethyl acetate (Fluka), toluene (Carlo Erba), chlorobenzene (Acros Organics), and hexane (Aldrich) were used as received. Acetonitrile (Carlo Erba) was distilled under Ar immediately before use from P_2O_5 . Tetrahydrofuran (THF) was purified by distillation from sodium/benzophenone under Ar immediately before use.

Moisture- and oxygen-sensitive reactions were carried out in flame-dried glassware under Ar. Column chromatography was carried out under positive pressure using 0.063–0.2 mm silica gel (Merck) and the indicated solvents. Evaporations were conducted under reduced pressure at temperatures lower than 45 °C. Further drying of the residues was accomplished under high vacuum. FT-IR spectra were recorded using a Perkin-Elmer Paragon 500 spectrometer. NMR spectra were run on a 200 MHz Bruker spectrometer. Liquid secondary ion mass spectrometry low- and high-resolution data (LSIMS, HRMS) were obtained from the mass spectrometry laboratory of the CRMPO at the University of Rennes 1, Rennes, France. MALDI data were recorded using a Bruker Daltonics Ultraflex MALDI-TOF/TOF. UV/vis spectra were recorded using a Bio-Tek Instruments UVIKON XS spectrometer. Fluorescence spectra were recorded using a Hitachi F-4500 fluorescence spectrophotometer. Analytical size exclusion chromatography (SEC) characterization was performed on an 1100 HP Chemstation equipped with a 300 mm \times 7.5 mm PLgel Mixed-D 5 μm 10^4 Å column (Polymer Laboratories), a UV/vis diode-array detector, and a refractive index detector. The calibration curve was obtained using ten monodisperse polystyrene (PS) narrow standards (S-M2-10 kit from Polymer Laboratories). Dilute solutions (20 μL) of PBTC (0.5 mg/mL) in HPLC-grade tetrahydrofuran (THF, Acros) were analyzed with UV–vis detection at 385 nm.

Cyclic Voltammetry and Differential Pulse Voltammetry. Cyclic voltammetry and differential pulse voltammetry experiments were carried out in a one-compartment electrolytic cell

containing a 0.1 M tetrabutylammonium perchlorate (NBu_4ClO_4)/ CH_2Cl_2 or acetonitrile electrolytic solution. The potentiostat used was an Autolab PGSTAT302, interfaced to a PC computer. The working electrode was a platinum disk (0.785 mm² area) or an ITO/glass slide (2 cm² area). A platinum wire was used as the counter electrode and silver (Ag) wire or Ag/AgCl as a reference electrode. The reference was calibrated after each experiment against the ferrocene/ferrocenium couple ($E_{\text{Fc}^+/\text{Fc}}^0 = 0.43$ V vs the Ag/AgCl reference) as recommended by IUPAC.²¹ The energy level of Fc^+/Fc is 4.8 eV below vacuum.²²

Monomer Synthesis. 3,6-Dibromocarbazole (2).²³ Carbazole (1) (501 mg, 3.0 mmol) was dissolved in CH_2Cl_2 (105 mL). SiO_2 (10 g) (0.063–0.2 nm, dried beforehand at 120 °C) was added. *N*-Bromosuccinimide (NBS) (1.07 g, 6.0 mmol) was then added slowly. The reaction mixture was stirred overnight at room temperature in the absence of light under argon atmosphere. The mixture was filtered and the silica washed with CH_2Cl_2 (3 \times 15 mL). The combined layers were washed with brine (3 \times 15 mL), dried over Na_2SO_4 , filtered, and evaporated to give **2** as a brown solid (786 mg, 80%): ¹H NMR (acetone-*d*₆, 200 MHz) δ 7.50 (dd, $J = 0.8$, 8.6 Hz, 2H), 7.55 (dd, $J = 1.7$, 8.6 Hz, 2H), 8.37 (dd, $J = 0.8$, 1.7 Hz, 2H), 10.66 (bs, 1H); ¹³C NMR (acetone-*d*₆, 50.3 MHz) δ 141.0, 130.8, 125.8, 125.1, 114.8, 113.4; LSIMS m/z (rel. intensity) 326 ($[\text{M} - \text{H}^+]$, 53), 324 ($[\text{M} - \text{H}^+]$, 100), 322 ($[\text{M} - \text{H}^+]$, 60).

***N*-(Ethylhexanoate)-3,6-dibromocarbazole (3).**²⁴ 3,6-Dibromocarbazole (**2**) (5.63 g, 17.31 mmol) was dissolved in DMF (35 mL). NaH (1.80 g, 75.00 mmol) was added slowly, and the solution was stirred under Ar at 50 °C for 1 h. Ethyl-6-bromohexanoate (5.1 mL, 28.56 mmol) was added dropwise. The reaction mixture was stirred at 80 °C for two days under Ar in the absence of light. DMF was evaporated; the mixture was dissolved in THF (35 mL) and Et_2O (30 mL) and washed with NH_4Cl (3 \times 40 mL), NaHCO_3 (40 mL), brine (50 mL), and water (2 \times 40 mL); and the organic phase was dried over Na_2SO_4 , filtered, and evaporated. The residue was purified by column chromatography, eluting with hexane/AcOEt (4:1) to afford **3** as a brown oil (4.51 g, 56%): ¹H NMR (CDCl_3 , 200 MHz) δ 8.16 (d, $J = 1.9$ Hz, 2H), 7.56 (dd, $J = 1.9$, 8.9 Hz, 2H), 7.28 (d, $J = 8.6$ Hz, 2H), 4.25 (t, $J = 7.0$ Hz, 2H), 4.12 (m, 2H), 2.29 (t, $J = 7.3$ Hz, 2H), 1.88 (m, 2H), 1.68 (m, 2H), 1.42 (m, 2H), 1.26 (t, $J = 7.0$ Hz, 3H); ¹³C NMR (CDCl_3 , 50.3 MHz) δ 173.4, 139.2, 129.0, 123.4, 123.2, 111.9, 110.3, 60.3, 43.0, 33.9, 28.5, 26.6, 24.5, 14.2; LSIMS m/z (rel. intensity) 470.0 ($[\text{M} - \text{H}^+]$, 51), 469.0 ($[\text{M}^+]$, 35), 468.0 ($[\text{M} - \text{H}^+]$, 100), 467.0 ($[\text{M}^+]$, 48), 466.0 ($[\text{M} - \text{H}^+]$, 53), 465.0 ($[\text{M}^+]$, 23); HRMS (FAB) m/z calcd for $\text{C}_{20}\text{H}_{21}\text{NO}_2\text{Br}_2\text{Na}$ 487.9836, found 487.9811.

***N*-(Ethylhexanoate)-3,6-bis(thiophen-2-yl)carbazole (4).**²⁵ *N*-(Ethylhexanoate)-3,6-dibromocarbazole (**3**) (1.36 g, 2.91 mmol) and thiophene-2-boronic acid (0.82 g, 6.41 mmol) were dissolved in THF (20 mL). Na_2CO_3 aqueous solution (2 M, 5.7 mL, 11.37 mmol) and $\text{Pd}(\text{PPh}_3)_4$ (0.14 g, 0.12 mmol) were added. The mixture was stirred and refluxed under Ar for 24 h. Water (80 mL) and CH_2Cl_2 (80 mL) were added. The organic phase was separated, washed with water (80 mL) and brine (65 mL), dried over Na_2SO_4 , filtered, and evaporated. The residue was purified by column chromatography, eluting with hexane/ CH_2Cl_2 (4:1, 2:1, 1:1, 1:2) to afford **4** as a light yellow-green oil (0.95 g, 69%): IR 2926, 2850, 2356, 1724, 1480, 1346, 1288, 1154, 1020, 798, 688 cm^{-1} ; ¹H NMR (CDCl_3 , 200 MHz) δ 8.38 (d, $J = 2.0$ Hz, 2H), 7.77 (dd, $J = 1.9$, 8.6 Hz, 2H), 7.42–7.38 (m, 4H), 7.31 (dd, $J = 1.3$, 5.1 Hz, 2H), 7.16 (dd, $J = 3.5$, 5.1 Hz, 2H), 4.32 (t, $J = 7.2$ Hz, 2H), 4.14 (m, 2H), 2.31 (t, $J = 7.3$

Hz, 2H), 1.94 (m, 2H), 1.71 (m, 2H), 1.44 (m, 2H), 1.26 (t, $J = 7.2$ Hz, 3H); ^{13}C NMR (CDCl_3 , 50.3 MHz) δ 173.4, 145.5, 140.3, 128.0, 125.9, 124.6, 123.7, 123.2, 122.1, 118.0, 109.1, 60.3, 43.0, 34.0, 28.7, 26.7, 24.6, 14.2; LSIMS m/z (rel. intensity) 496.1 ($[\text{M} - \text{Na}^+]$, 100), 473.2 ($[\text{M} - \text{H}^+]$, 35); HRMS (FAB) m/z calcd for $\text{C}_{28}\text{H}_{27}\text{NO}_2\text{S}_2$ 473.1483, found 473.1472.

***N*-(Hexan-6-ol)-3,6-bis(thiophen-2-yl)carbazole (5).** *N*-(Ethylhexanoate)-3,6-bis(thiophen-2-yl)carbazole (**4**) (0.88 g, 1.86 mmol) was dissolved in THF (22 mL) at -60°C . LiAlH_4 1 M in THF (5 mL, 5 mmol) was added dropwise. The reaction was stirred under Ar at a temperature below -40°C for 50 min. HCl 2 M (2 mL) and water (5 mL) were added. The solution was dissolved in Et_2O (50 mL), and the organic phase was washed with water (5×30 mL), dried over Na_2SO_4 , filtered, and evaporated to afford **5** as a light yellow-green solid (0.71 g, 87%): ^1H NMR (CDCl_3 , 200 MHz) δ 8.36 (d, $J = 1.4$ Hz, 2H), 7.76 (dd, $J = 1.7$, 8.5 Hz, 2H), 7.42–7.36 (m, 4H), 7.29 (dd, $J = 1.0$, 4.6 Hz, 2H), 7.14 (dd, $J = 3.5$, 5.1 Hz, 2H), 4.32 (t, $J = 7.0$ Hz, 2H), 3.62 (t, $J = 6.0$ Hz, 2H), 1.89 (m, 2H), 1.55 (m, 2H), 1.42 (m, 4H); ^{13}C NMR (CDCl_3 , 50.3 MHz) δ 145.6, 140.4, 128.0, 125.9, 124.6, 123.7, 123.2, 122.1, 118.0, 109.1, 62.7, 43.2, 32.5, 29.0, 27.0, 25.5; LSIMS m/z (rel. intensity) 431.1 ($[\text{M}^{++}]$, 40), 432.1 ($[\text{M} - \text{H}^+]$, 100); HRMS (ESI) m/z calcd for $\text{C}_{26}\text{H}_{25}\text{NOS}_2\text{K}$ ($[\text{M} - \text{K}^+]$) 470.1014, found 470.1031.

***N*-(6-Bromohexane)-3,6-bis(thiophen-2-yl)carbazole (6).** *N*-(Hexan-6-ol)-3,6-bis(thiophen-2-yl)carbazole (**5**) (44.0 mg, 0.10 mmol) was dissolved in toluene (4 mL). HBr (48%, 0.55 mL, 4.90 mmol) was added dropwise. The reaction was stirred and refluxed overnight under Ar in the absence of light. Toluene (35 mL) and water (30 mL) were added. The organic phase was washed with water (25 mL), brine (2×30 mL), and water (2×30 mL), dried over Na_2SO_4 , filtered, and evaporated. The residue was purified by column chromatography, eluting with hexane/ CH_2Cl_2 (2:1) to afford **6** as a green oil (21.5 mg, 43%): ^1H NMR (CDCl_3 , 200 MHz) δ 8.35 (d, $J = 1.4$ Hz, 2H), 7.75 (dd, $J = 1.8$, 8.5 Hz, 2H), 7.41–7.36 (m, 4H), 7.28 (dd, $J = 1.2$, 5.2 Hz, 2H), 7.12 (dd, $J = 3.5$, 5.1 Hz, 2H), 4.32 (t, $J = 6.9$ Hz, 2H), 3.37 (t, $J = 6.6$ Hz, 2H), 1.86 (m, 2H), 1.46 (m, 6H); ^{13}C NMR (CDCl_3 , 50.3 MHz) δ 145.6, 140.4, 128.0, 126.0, 124.7, 123.8, 123.2, 122.2, 118.0, 109.1, 43.1, 33.7, 32.5, 28.9, 27.9, 26.4; LSIMS m/z (rel. intensity) 493.0 ($[\text{M}^{++}]$, 38), 494.0 ($[\text{M} - \text{H}^+]$, 94), 495.0 ($[\text{M} - \text{H}^+]$, 70), 496.0 ($[\text{M} - \text{H}^+]$, 100); HRMS (ESI) m/z calcd for $\text{C}_{26}\text{H}_{24}\text{NBrS}_2\text{Na}$ ($[\text{M} - \text{Na}^+]$) 516.0431, found 516.0409.

***N*-(6-Azohexane)-3,6-bis(thiophen-2-yl)carbazole (7).** *N*-(6-Bromohexane)-3,6-bis(thiophen-2-yl)carbazole (**6**) (22.9 mg, 0.046 mmol) was dissolved in DMF (10 mL). NaN_3 (37.1 mg, 0.57 mmol) was added. The reaction mixture was stirred overnight at 85°C under Ar in the absence of light. Water (20 mL) and CH_2Cl_2 (25 mL) were added. The organic phase was washed with brine (2×25 mL) and water (2×25 mL), dried over Na_2SO_4 , filtered, and evaporated to afford **7** as a yellow oil (20.8 mg, 99%): IR 2918, 2850, 2350, 2093, 1728, 1596, 1476, 1248, 1218, 792, 688 cm^{-1} ; ^1H NMR (CDCl_3 , 200 MHz) δ 8.35 (d, $J = 1.8$ Hz, 2H), 7.74 (dd, $J = 1.8$, 8.5 Hz, 2H), 7.39–7.34 (m, 4H), 7.27 (dd, $J = 1.2$, 6.3 Hz, 2H), 7.12 (dd, $J = 3.5$, 5.1 Hz, 2H), 4.29 (t, $J = 7.0$ Hz, 2H), 3.22 (t, $J = 6.5$ Hz, 2H), 1.90 (m, 2H), 1.52 (m, 2H), 1.40 (m, 4H); ^{13}C NMR (CDCl_3 , 50.3 MHz) δ 145.5, 140.3, 128.0, 126.0, 124.6, 123.7, 123.2, 122.1, 118.0, 109.1, 51.3, 43.1, 29.4, 28.7, 26.8, 26.5; LSIMS m/z (rel. intensity) 456.17 ($[\text{M}^{++}]$, 100), 457.17 ($[\text{M} - \text{H}^+]$, 95).

***N*-(6-Azafullerohexane)-3,6-bis(thiophen-2-yl)carbazole (BTC-F).**²⁶ C_{60} (197.7 mg, 0.27 mmol) was dissolved in chlorobenzene (50 mL). *N*-(6-Azohexane)-3,6-bis(thiophen-2-yl)carbazole (**7**) (64.0 mg, 0.14 mmol) dissolved in chlorobenzene (15 mL) was added. The reaction mixture was stirred at 130°C for two days under Ar in the absence of light. Chlorobenzene was evaporated, and THF was added to the residue. The solution was stirred for 3 h. The unreacted C_{60} was filtered off, and the filtrate was evaporated to afford BTC-F as a dark brown powder (147.1 mg, 91%): IR 2916, 2850, 2340, 1736, 1452, 1425, 1371, 1191, 1084, 1029, 794, 737, 688 cm^{-1} ; ^1H NMR ($\text{C}_2\text{D}_2\text{Cl}_4$, 200 MHz) δ 8.31 (d, $J = 1.6$ Hz, 2H), 7.74 (dd, $J = 1.6$, 8.9 Hz, 2H), 7.47–7.35 (m, 4H), 7.28 (dd, $J = 1.3$, 5.1 Hz, 2H), 7.11 (dd, $J = 3.5$, 5.1 Hz, 2H), 4.34 (t, $J = 7.0$ Hz, 2H), 3.70 (t, $J = 7.0$ Hz, 2H), 2.00 (m, 2H), 1.57 (m, 2H), 1.34 (m, 4H); MALDI (EI) m/z calcd for $\text{C}_{86}\text{H}_{24}\text{N}_2\text{S}_2$ 1148.1380, found 1148.1293.

Polymer Electrosynthesis. ***Poly*(*N*-(ethylhexanoate)-3,6-bis(thiophen-2-yl)carbazole) (PBTC).** The oxidative electrochemical polymerization of monomer **4** was carried out by cyclic voltammetry at a concentration of 2.8 mM in MeCN containing NBu_4ClO_4 (0.1 M) at a scan rate of $50 \text{ mV} \cdot \text{s}^{-1}$ (10 repeated scans) to form a film which is yellow in the neutral state. A Ag/AgCl sat. electrode was used as the reference electrode. A platinum disk and ITO (indium–tin–oxide) glass were used as the working electrode.

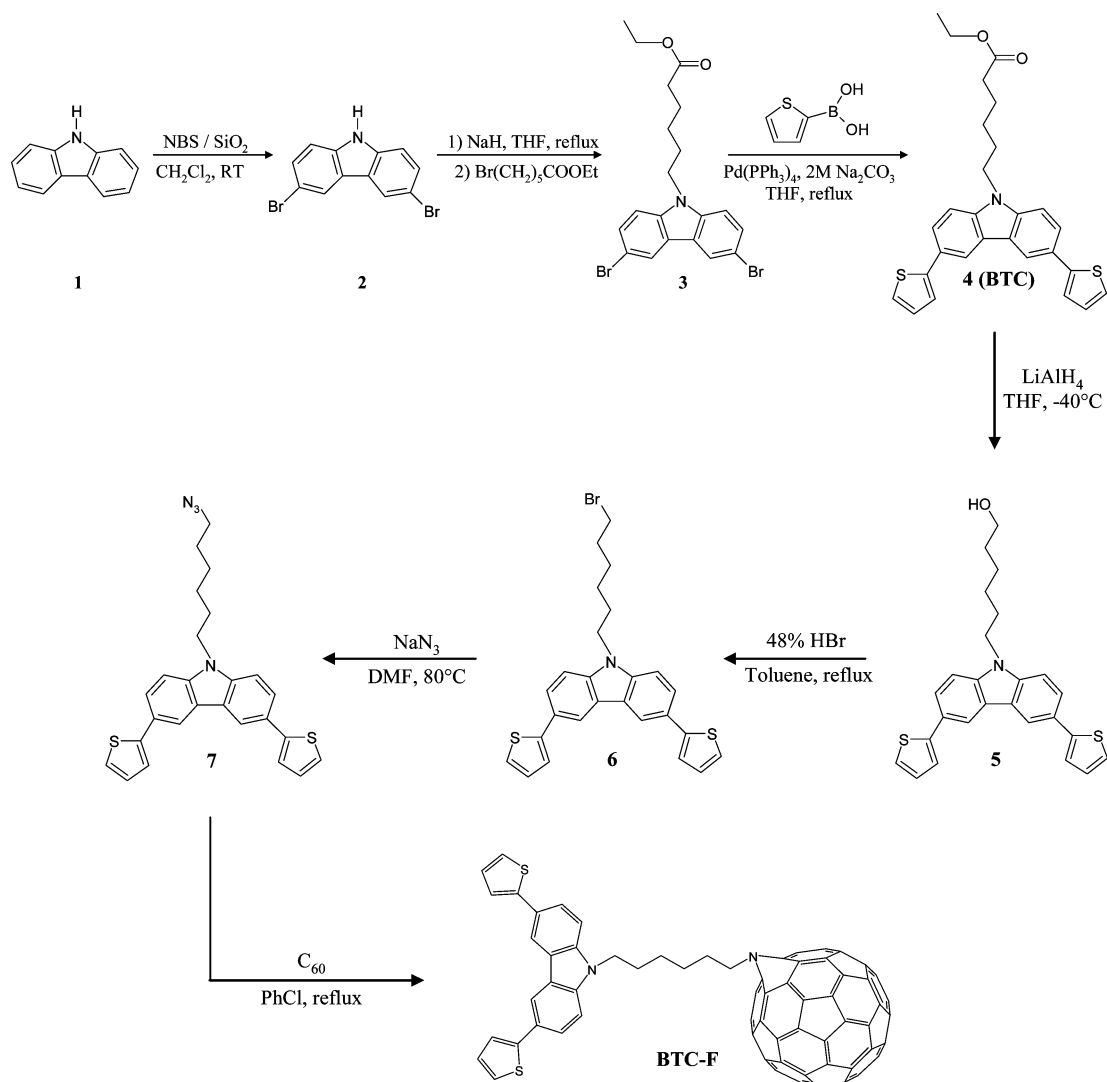
***Poly*(*N*-(6-fullerohexane)-3,6-bis(thiophen-2-yl)carbazole) (PBTC-F).** The oxidative electrochemical polymerization of BTC-F was carried out by cyclic voltammetry at a concentration of 0.08 mM in CH_2Cl_2 containing NBu_4ClO_4 (0.1 M) at a scan rate of $50 \text{ mV} \cdot \text{s}^{-1}$ (10 repeated scans) to form a brown film. A silver wire was used as a pseudoreference electrode. Platinum disk and ITO (indium–tin–oxide) glass were used as a working electrode.

Results and Discussion

Synthesis and Characterization of BTC-F. The synthesis route to the C_{60} -functionalized bisthiophene-carbazole is shown in Scheme 2. Commercially available carbazole **1** was dibrominated at room temperature by use of two equivalents of *N*-bromosuccinimide (NBS) in the presence of silica. In such conditions, bromination occurs on the 3 and 6 positions of carbazole to afford 3,6-dibromocarbazole (**2**) in good yield (80%). **2** was *N*-alkylated with an alkyl chain bearing an ester function. The nitrogen atom of the carbazole moiety was first deprotonated using NaH before introducing ethyl-6-bromohexanoate in the reaction mixture. *N*-(Ethylhexanoate)-3,6-dibromocarbazole (**3**) was obtained in reasonable yield (56%). The alkyl chain acts as a protector group for the nitrogen atom of the carbazole during the next reaction. The coupling of thiophene was performed through a Suzuki coupling reaction with thiophene-2-boronic acid using $\text{Pd}(\text{PPh}_3)_4$ as a catalyst and an aqueous solution of Na_2CO_3 as a base. *N*-(Ethylhexanoate)-3,6-bis(thiophen-2-yl)carbazole (**4**) was obtained in 69% yield. The presence of an alkyl chain on the carbazole increases the solubility of the molecule. Compound **2** is hardly soluble in chloroform, while **3** and **4** are soluble in all common organic solvents such as CH_2Cl_2 , THF, MeCN, acetone, or chloroform.

The chemical transformation of the ester group of **4** (BTC) into an azide group allows the grafting of C_{60} . The reaction of C_{60} with the azide function is known to proceed through monoaddition and leads to aza-bridged fullerenes.²⁶ Compound **5** was obtained by reduction of the ester group of **4** using LiAlH_4 (87% yield) and was brominated with HBr to get **6** in 43% yield. The conversion of the bromine to the azide group with NaN_3

SCHEME 2: Synthesis Reaction Scheme of the BTC-F Dyad



gives the azide-functionalized bithiophene-carbazole **7** in 99% yield. Fullerene C₆₀ was grafted onto **7**. The grafted bithiophene-carbazole monomer (BTC-F) was separated from the unreacted C₆₀ by dissolution of the residue of the reaction in THF, in which C₆₀ is insoluble,²⁷ followed by filtration. After purification, BTC-F was obtained in good yield (91% based on monomer **7**).

Due to its low solubility, no ¹³C NMR spectrum of BTC-F was recorded. A comparison of the FTIR spectrum of BTC-F with those of **4** and **7** (Figure 1) clearly shows the disappearance of the absorption band characteristic of the azide group at 2093 cm⁻¹.

Optical Properties of BTC-F. UV-vis spectroscopy is a very sensitive tool for the study of fullerenes and conjugated polymers functionalization, and for this reason it is very suitable for investigating BTC-F. In particular, it is instructive to compare spectral features of this molecule with those obtained for BTC alone (see Figure 2a). Pure BTC gives a band peaking at 310 nm with no significant absorbance beyond 390 nm. For BTC-F, the spectrum is dominated by a band at 330 nm originating from the fullerene moiety.²⁸ It should also be noted that two broad bands at 540 and 600 nm appear in the case of BTC-F (see the inset in Figure 2a). These spectral bands originate from the broken symmetry of the functionalized fullerene as compared to its initial I_h point group and are

characteristic of iminofullerenes.²⁸ Thus, the observed spectral changes can be taken as a spectroscopic manifestation of the grafting of the fullerene moiety to BTC.

The next question to be answered, which is of crucial importance, is how the grafting reaction influences the efficiency of the quenching of the photoluminescence in the obtained hybrid (BTC-F). Effective luminescence quenching constitutes a *condition sine qua non* for potential application of BTC-F in solar cells. Photoluminescence spectra of BTC and BTC-F are

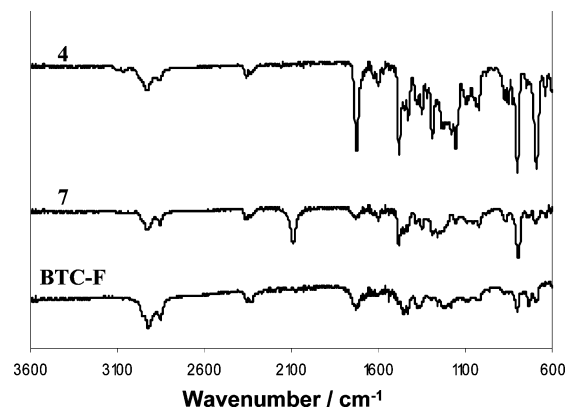


Figure 1. FT-IR spectra of monomers **4**, **7**, and BTC-F.

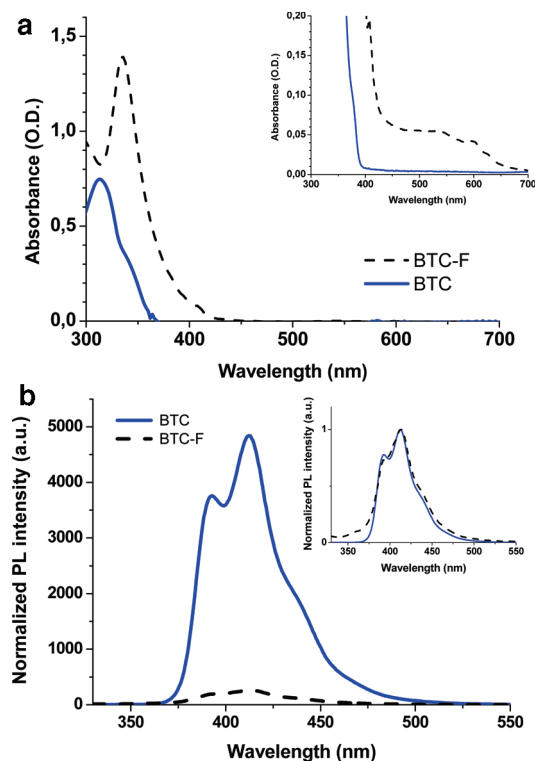


Figure 2. (a) UV/vis absorption spectra of monomers BTC (solid line) and BTC-F (dashed line) diluted in toluene at a concentration of $2.5 \times 10^{-5} \text{ mol} \cdot \text{L}^{-1}$. The inset shows a magnified view of the spectra in the spectral range 400–700 nm. In this case, the measurements were performed at a concentration of $5 \times 10^{-5} \text{ mol} \cdot \text{L}^{-1}$ to improve the signal-to-noise ratio. (b) Photoluminescence spectra of BTC (solid line) and BTC-F (dashed line). The measurements were performed in toluene at an excitation wavelength $\lambda_{\text{exc}} = 310 \text{ nm}$ corresponding to the maximum of absorption of the BTC moiety.

almost identical in shape as can be seen in the inset of Figure 2b, and therefore they must be attributed to the BTC molecule. Nevertheless, the presence of the grafted fullerene moieties in the case of BTC-F induces a strong quenching of the BTC photoluminescence indicating a photoinduced charge transfer between the BTC moiety and the fullerene one. Again, this effective quenching can be considered as an indirect evidence of the fullerene grafting reaction.

PBTC and PBTC-F Films. Electrochemical oxidative-type polymerization enables facile preparation of double-cable polymer films of PBTC-F with one fullerene moiety per bisthiophene-carbazole repeat unit corresponding to 63 wt % proportion of fullerene. This is significantly higher than what can be achieved by chemical polymerization. To elucidate the effect of fullerene grafting on the electropolymerization process, we have comparatively studied electrochemical polymerization of BTC and BTC-F on ITO/glass slides as a substrate. Both monomers were electropolymerized by cyclic voltammetry on a platinum working electrode in 0.1 M NBu_4ClO_4 acetonitrile (Figure 3). Electrochemical growth of the polymers starts with the first cycle. The onset of the oxidative polymerization potential occurs at 0.46 and 0.39 V for BTC and BTC-F, respectively. During the growth of the BTC-F film, a new redox couple appears at lower potentials (at $E_{\text{ox}} = 0.40 \text{ V}$ and $E_{\text{red}} = 0.32 \text{ V}$) which can be attributed to oxidative-type doping (i.e., polarons and/or bipolarons formation) and reductive dedoping of the formed polymer.

Although insoluble in acetonitrile, PBTC films are soluble in common organic solvents such as CH_2Cl_2 , CHCl_3 , THF, and

toluene. Size-exclusion chromatography gave $M_n = 2980 \text{ Da}$ with a polydispersity index (PDI) of 1.42. This corresponds to a degree of polymerization (DP_n) of ca. 6. Although it was not possible to determine the M_n value of PBTC-F, due to its insolubility, a comparison of the UV–vis absorption spectrum of a thin film of PBTC-F with that of PBTC can shine light on the polymerization degree of the hybrid polymer (see Figure 4). It can be noticed that in the case of PBTC-F the maximum of its $\pi-\pi^*$ transition peak (at 436 nm) shows a small bathochromic shift of approx 30 nm as compared to the maximum of the analogous peak in PBTC. Since the energy of the $\pi-\pi^*$ transition decreases with increasing DP_n ,²⁹ it may be concluded that the chains of PBTC-F are slightly longer than those of PBTC. This means that bulky fullerene moieties do not impede the electropolymerization, provided that they are separated from the bisthiophene-carbazole monomer by a sufficiently long, flexible spacer.

The onset of the $\pi-\pi^*$ transition peak in the UV–vis spectrum of PBTC at approximately 490 nm corresponds to an optical gap of 2.52 eV, in good agreement with the optical gap of a similar polybisthiophene-carbazole already reported.³⁰ Similar calculation for PBTC-F is not possible due to the long wavelength tail which obscures the onset of the polymer $\pi-\pi^*$ transition band. The presence of fullerenes in PBTC-F is evidenced in its absorption spectrum by a higher absorbance at wavelengths below 400 nm and by the long wavelength tail of the $\pi-\pi^*$ transition peak, although some contribution of scattering effects for this part of the spectrum cannot be totally excluded.

BTC-F and PBTC-F Electronic Levels. Cyclic voltammetry is a useful electrochemical technique to determine the redox properties and electronic energy levels of conjugated polymers.³¹ In this respect, differential pulse voltammetry (DPV) is even more advantageous because it eliminates the capacitive response of the electrode.³² BTC-F and PBTC-F were electrochemically characterized by cyclic voltammetry and differential pulse voltammetry with the goal to measure their electronic levels (Figure 5). For comparison, C_{60} and PCBM were also studied using the same electrochemical conditions.

The BTC-F voltammograms, in their reductive part, show three quasi-reversible peaks (Figure 5a and 5c). It is well-known that fullerene molecules can form multiply charged anions during reduction.³³ The values of the reduction peaks for BTC-F were found to be more negative than those of C_{60} and PCBM (Table 1). The LUMO level can be deduced from the first reduction potential. For BTC-F, the values of the first reduction potential measured by CV and DPV were very close (−1.11 and −1.12 V, respectively). As the redox couple ferrocenium/ferrocene (Fc^+/Fc) was the reference in our measurements, the following expression can be used to calculate the position in energy relative to vacuum level of the reduction (oxidation) peaks in the voltammograms³⁴

$$E_{\text{level}} (\text{eV}) = -4.8 - E_{\text{peak}}$$

The LUMO energy level of BTC-F is therefore ca. −3.7 eV vs vacuum, i.e., slightly higher than the measured LUMO levels of C_{60} and of the commonly used PCBM acceptor. It is worth mentioning that raising the LUMO of the acceptor allows higher V_{oc} in solar cell devices.⁸ Therefore, using BTC-F as an alternative electron acceptor to PCBM in polycarbazole-based solar cell devices might help improve V_{oc} and therefore the efficiency of the devices.³⁵ The LUMO level of BTC-F is similar to the one of a bis-PCBM acceptor that exhibited a significantly

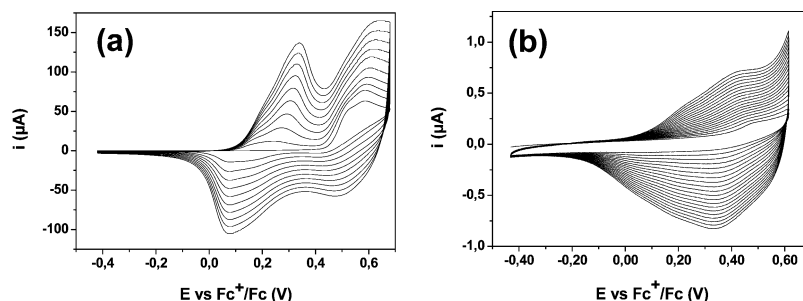


Figure 3. (a) Electropolymerization of BTC by cyclic voltammetry at a concentration of 2.8 mM in acetonitrile containing 0.1 M NBu_4ClO_4 at a Pt working electrode, $\nu = 50 \text{ mV} \cdot \text{s}^{-1}$. (b) Electropolymerization of 0.08 mM BTC-F by cyclic voltammetry in dichloromethane containing 0.1 M NBu_4ClO_4 at a Pt working electrode, $\nu = 50 \text{ mV} \cdot \text{s}^{-1}$, Ag wire reference electrode.

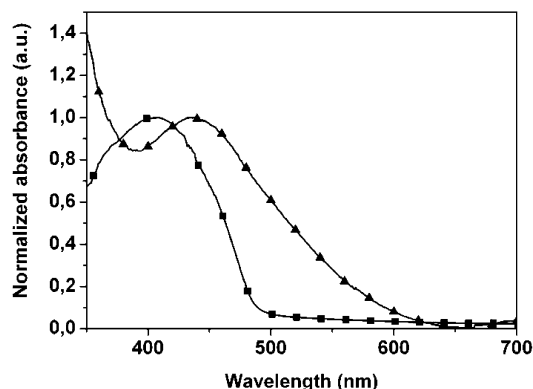


Figure 4. Normalized UV/vis absorption spectra of a PBTC film (squares) and a PBTC-F film (triangles) electrodeposited on ITO/glass substrate.

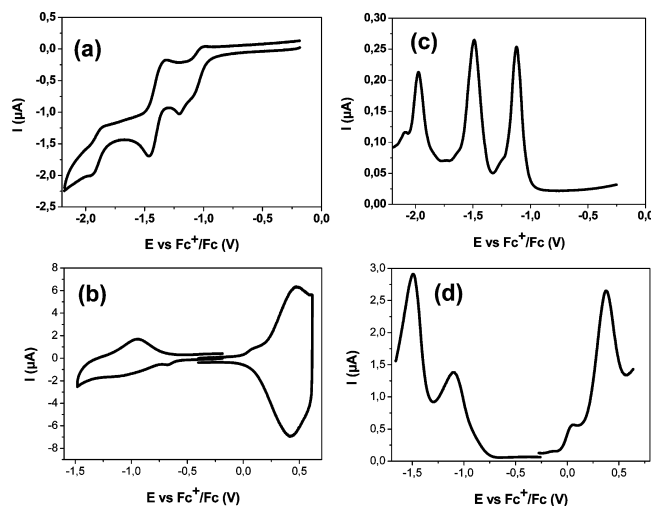


Figure 5. Cyclic voltammograms of (a) BTC-F at a concentration of 0.08 mM in CH_2Cl_2 containing 0.1 M NBu_4ClO_4 , Pt working electrode, $\nu = 50 \text{ mV} \cdot \text{s}^{-1}$, and (b) PBTC-F film on a Pt working electrode in acetonitrile containing 0.1 M NBu_4ClO_4 , $\nu = 50 \text{ mV} \cdot \text{s}^{-1}$. Differential pulse voltammetry of (c) BTC-F at a concentration of 0.08 mM in CH_2Cl_2 containing 0.1 M NBu_4ClO_4 , Pt working electrode, $\nu = 10 \text{ mV} \cdot \text{s}^{-1}$, and (d) PBTC-F film on a Pt working electrode in acetonitrile containing 0.1 M NBu_4ClO_4 , $\nu = 10 \text{ mV} \cdot \text{s}^{-1}$.

improved V_{oc} when blended with P3HT.³⁶ The voltammogram of BTC-F in the oxidative region can be seen in Figure 3 during the first cycle by CV as subsequent cycles lead to electropolymerization and formation of a film of PBTC-F. From this voltammogram, the oxidation peak position $E_{1/2\text{ox}}^1$ was determined to be 0.48 V (vs Fc^+/Fc) corresponding to a HOMO energy level of -5.28 eV (vs vacuum).

Redox potentials of PBTC-F were also measured (Figure 5b and 5d). The oxidation of PBTC-F is characterized by a redox

TABLE 1: Redox Potentials^a versus Fc^+/Fc for Compounds in This Study

compd	CV				DPV			
	$E_{1/2\text{red}}^1$	$E_{1/2\text{red}}^2$	$E_{1/2\text{red}}^3$	$E_{1/2\text{ox}}^1$	E_{red}^1	E_{red}^2	E_{red}^3	E_{ox}^1
C_{60}	-1.02	1.42	-1.87	1.30	-1.01	-1.42	-1.90	1.22
PCBM	-1.05	-1.45	-1.98	1.12	-1.06	-1.47	-1.99	1.07
BTC-F	-1.11	-1.46	-1.97	0.48	-1.12	-1.51	-1.99	N/A
PBTC-F	-0.91	N/A	N/A	0.43	-1.10	-1.49	N/A	0.37

^a CV $E_{1/2}$ redox potentials are calculated as $0.5(E_{\text{pa}} + E_{\text{pc}})$ in V vs Fc^+/Fc .

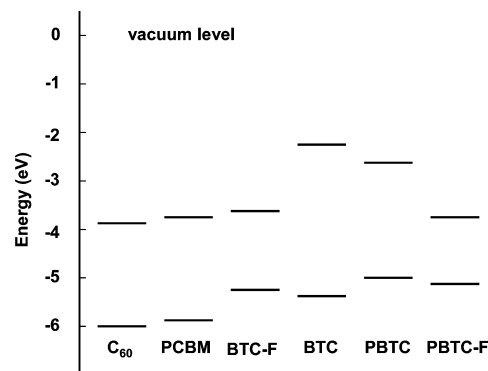


Figure 6. HOMO and LUMO levels of C_{60} , PCBM, BTC-F, BTC, PBTC, and PBTC-F. The LUMO level of BTC was obtained from its HOMO level and its optical bandgap.

potential at 0.43 V by CV and 0.37 V by DPV corresponding to the p-doping of the polymer. Taking the latter value as more precise, we estimate the HOMO level of PBTC-F as -5.2 eV . A small prepeak observed at 0.05 V can be attributed to residual charges inside the polymer film.³⁷ The cyclic voltammogram also shows a poorly resolved set of quasi-reversible reduction peaks corresponding to the reduction of the fullerene moiety (Figure 5c). DPV measurements were necessary to observe the first two reduction peaks. The values of the reduction potentials of the fullerene component in BTC-F and PBTC-F were found to be very close, indicating that the electronic properties of the grafted fullerene moieties remain in the double-cable polymer.

The data from the CV and DPV measurements are summarized in Table 1. These measurements combined with the spectroscopic studies allow us to establish the relative HOMO/LUMO energy level diagram for the different compounds studied in this work (Figure 6). At first, it can be noticed that the relative position of the HOMO/LUMO energy levels for BTC and C_{60} is in favor of intramolecular charge transfer, in accordance with the photoluminescence quenching observed for BTC-F (see Figure 2b). The same remark applies to PBTC and C_{60} which makes this donor/acceptor couple and the derived double-cable polymer PBTC-F good candidates for photovoltaic

applications. Moreover, the observed HOMO–LUMO bandgap of PBTC-F (BTC-F) appears to be a combination of the HOMO of PBTC (BTC) and of the LUMO of C₆₀. The energy difference between these levels for PBTC-F (as measured by DPV) is 1.47 eV. As the V_{oc} in solar cell devices is directly proportional to this difference, this demonstrates the potential of thiophene-carbazole-based polymers and derived double-cable polymers to lead to solar cell devices with higher V_{oc} compared to P3HT-based devices.

Conclusions

To summarize, we have synthesized a new donor–acceptor dyad, namely, a 3,6-bis(thiophen-2-yl)carbazole derivative bearing a C₆₀ fullerene as a side group (BTC-F). Spectroscopic measurements carried out for BTC-F indicate that fullerene grafting induces effective quenching of the BTC photoluminescence by the fullerene moiety. The monomer BTC-F can be electrochemically polymerized to give a double cable-type polymer (PBTC-F) with a high content of fullerenes (63 wt %). Electrochemically determined LUMO energy level of the fullerene component of both hybrids (BTC-F and PBTC-F) is slightly higher than that of unmodified fullerene or PCBM. Moreover, it was demonstrated that PBTC-F exhibits a high donor HOMO–acceptor LUMO gap and is therefore likely to help increase the V_{oc} if used in organic solar cells. The photovoltaic properties of such materials are currently under investigation.

Acknowledgment. We are grateful to Dr. Patrice Rannou for his assistance with SEC analysis. Stimulating discussions with Pr. Adam Pron, Dr. David Djurado, Dr. Frédéric Lincker, and Julien Danet are also gratefully acknowledged.

References and Notes

- (1) (a) Gaupp, C. L.; Reynolds, J. R. *Macromolecules* **2003**, *36*, 6305–6315. (b) Sotzing, G. A.; Reddinger, J. L.; Katritzky, A. R.; Soloducho, J.; Musgrave, R.; Reynolds, J. R. *Chem. Mater.* **1997**, *9*, 1578–1587. (c) Reddinger, J. L.; Sotzing, G. A.; Reynolds, J. R. *Chem. Commun.* **1996**, *15*, 1777–1778. (d) Tran-Van, F.; Henri, T.; Chevrot, C. *Electrochim. Acta* **2002**, *47*, 2927. (e) Chevrot, C.; Ngbi, E.; Kham, K.; Sadki, S. *Synth. Met.* **1996**, *81*, 201–204.
- (2) Aich, R. B.; Blouin, N.; Bouchard, A.; Leclerc, M. *Chem. Mater.* **2009**, *21*, 751–757.
- (3) Morin, J. F.; Leclerc, M.; Ades, D.; Siove, A. *Macromol. Rapid Commun.* **2005**, *26*, 761–778.
- (4) Li, Y.; Ding, J.; Day, M.; Tao, Y.; Lu, J.; D'orio, M. *Chem. Mater.* **2004**, *16*, 2165–2173.
- (5) Yoshida, M.; Suemori, K.; Uemura, S.; Hoshino, S.; Kodzasa, T.; Kamata, T.; Kondo, T.; Kawai, H.; Kawai, T. *Mol. Cryst. Liq. Cryst.* **2007**, *471*, 21–27.
- (6) Wang, Y. *Nature* **1992**, *356*, 585–587.
- (7) Li, J.; Dierschke, F.; Wu, J.; Grimsdale, A. C.; Mullen, K. *J. Mater. Chem.* **2006**, *16*, 96–100.
- (8) (a) Brabec, C. J.; Cravino, A.; Meissner, D.; Sariciftci, N. S.; Fromherz, T.; Rispens, M. T.; Sanchez, L.; Hummelen, J. C. *Adv. Funct. Mater.* **2001**, *11*, 374–380. (b) Brabec, C. J.; Cravino, A.; Meissner, D.; Sariciftci, N. S.; Rispens, M. T.; Sanchez, L.; Hummelen, J. C.; Fromherz,

- T. *Thin Solid Films* **2002**, *403*, 368–372. (c) Gunes, S.; Neugebauer, H.; Sariciftci, N. S. *Chem. Rev.* **2007**, *107*, 1324–1338.
- (9) (a) Leclerc, N.; Michaud, A.; Sirois, K.; Morin, J. F.; Leclerc, M. *Adv. Funct. Mater.* **2006**, *16*, 1694–1704. (b) Blouin, N.; Michaud, A.; Leclerc, M. *Adv. Mater.* **2007**, *19*, 2995–3000. (c) Blouin, N.; Michaud, A.; Gendron, D.; Wakim, S.; Blair, E.; Neagu-Plesu, R.; Belletete, M.; Durocher, G.; Tao, Y.; Leclerc, M. *J. Am. Chem. Soc.* **2008**, *130*, 732–742. (d) Park, S. H.; Roy, A.; Beaupré, S.; Cho, S.; Coates, N.; Moon, J. S.; Moses, D.; Leclerc, M.; Lee, K.; Heeger, A. J. *Nat. Photonics* **2009**, *3*, 297–302.
- (10) Nunzi, J. M. C. R. *Physique* **2002**, *3*, 523–542.
- (11) Yassar, A.; Hmyene, H.; Loveday, D. C.; Ferraris, J. P. *Synth. Met.* **1997**, *84*, 231–232.
- (12) Cravino, A.; Sariciftci, N. S. *Nat. Mater.* **2003**, *2*, 360–361.
- (13) Roncali, J. *J. Chem. Soc. Rev.* **2005**, *34*, 483–495.
- (14) Tan, Z.; Hou, J.; He, Y.; Zhou, E.; Yang, C.; Li, Y. *Macromolecules* **2007**, *40*, 1868–1873.
- (15) Ouhib, F.; Khouch, A.; Ledeuil, J. B.; Martinez, H.; Desbrières, J.; Dagron-Lartigau, C. *Macromolecules* **2008**, *41*, 9736–9743.
- (16) Jousset, B.; Blanchard, P.; Levillain, E.; de Bettignies, R.; Roncali, J. *Macromolecules* **2003**, *36*, 3020–3025.
- (17) Blanco, R.; Gomez, R.; Seoane, C.; Segura, J. L.; Mena-Osteritz, E.; Bauerle, P. *Org. Lett.* **2007**, *9*, 2171–2174.
- (18) Kim, S. Y.; Lee, K. H.; Chin, B. D.; Yu, J. W. *Sol. Energy Mater. Sol. Cells* **2009**, *93*, 129–135.
- (19) Yang, C.; Li, H.; Sun, Q.; Qiao, J.; Li, Y.; Li, Y.; Zhu, D. *Sol. Energy Mater. Sol. Cells* **2005**, *85*, 241–249.
- (20) Giacalone, F.; Martin, N. *Chem. Rev.* **2006**, *106*, 5136–5190.
- (21) Schottland, P.; Zong, K.; Gaupp, C. L.; Thompson, B. C.; Thomas, C. A.; Giurgiu, I.; Hickman, R.; Abboud, K. A.; Reynolds, J. R. *Macromolecules* **2000**, *33*, 7051–7061.
- (22) Polec, I.; Henckens, A.; Goris, L.; Nicolas, M.; Loi, M. A.; Adriaenssens, P. J.; Lutsen, L.; Manca, J. V.; Vanderzande, D.; Sariciftci, N. S. *J. Polym. Sci., Part A: Polym. Chem.* **2003**, *41*, 1034–1045.
- (23) (a) Smith, K.; James, D. M.; Mistry, A. G.; Bye, M. R.; Faulkner, D. J. *Tetrahedron* **1992**, *48*, 7479–7488. (b) Fabre-Francke, I.; Zagorska, M.; Louarn, G.; Hapiot, P.; Pron, A.; Sadki, S. *Electrochim. Acta* **2008**, *53*, 6469–6476.
- (24) Zhang, Z. B.; Motonaga, M.; Fujiki, M.; McKenna, C. E. *Macromolecules* **2003**, *36*, 6956–6958.
- (25) Promarak, V.; Ruchirawat, S. *Tetrahedron Lett.* **2007**, *63*, 1602–1609.
- (26) Prato, M.; Li, Q. C.; Wudl, F.; Lucchini, V. *J. Am. Chem. Soc.* **1993**, *115*, 1148–1150.
- (27) Ruoff, R. S.; Tse, D. S.; Malhotra, R.; Lorents, D. C. *J. Phys. Chem.* **1993**, *97*, 3379–3383.
- (28) Yang, C.; Cho, S.; Heeger, A. J.; Wudl, F. *Angew. Chem., Int. Ed.* **2009**, *48*, 1–5.
- (29) Pokrop, R.; Verilhac, J. M.; Gasior, A.; Wielgus, I.; Zagorska, M.; Travers, J. P.; Pron, A. *J. Mater. Chem.* **2006**, *16*, 3099–3106.
- (30) Witker, D.; Reynolds, J. R. *Macromolecules* **2005**, *38*, 7636–7644.
- (31) Lyons, M. E. G. *Electroactive Polymer Chemistry. Part 1: Fundamentals*; Plenum Press: New York and London, 1994; p 145.
- (32) Bard, A. J.; Faulkner, L. R. *Electrochemical techniques, Fundamentals and Applications*, 2nd ed.; 2001; p 286.
- (33) Xie, Q. S.; Perez-Cordero, E.; Echegoyen, L. *J. Am. Chem. Soc.* **1992**, *114*, 3978–3980.
- (34) Polec, I.; Henckens, A.; Goris, L.; Nicolas, M.; Loi, M. A.; Adriaenssens, P. J.; Lutsen, L.; Manca, J. V.; Vanderzande, D.; Sariciftci, N. S. *J. Polym. Sci., Part A: Polym. Chem.* **2003**, *41*, 1034–1045.
- (35) Kooistra, F. B.; Knol, J.; Kastenberg, F.; Popescu, L. M.; Verhees, W. J. H.; Kroon, J. M.; Hummelen, J. C. *Org. Lett.* **2007**, *9*, 551–554.
- (36) Lenes, M.; Wetzelaer, G. J. A. H.; Kooistra, F. B.; Veenstra, S. C.; Hummelen, J. C.; Blom, P. W. M. *Adv. Mater.* **2008**, *20*, 2116–2119.
- (37) Ding, H.; Pigani, L.; Seiber, R.; Zanardi, C. *J. New Mater. Electrochem. Systems* **2000**, *3*, 339–343.

JP905876H